

# KRAS G12C as a Target of Naringenin for Inducing Cell Death in NCI-H23 Cells

Abani Kumar Patar, Lakhon Kma, Jitul Barman, Shekhar Ghosh, Taranga Jyoti Baruah\*

## ABSTRACT

**Background:** Naringenin (NGN) is a commonly available flavonoid in the citrus fruits. We have previously shown that NGN is cytotoxic to the non-small cell lung cancer (NSCLC) cell line NCI-H23 (H23). **Objectives:** To check whether NGN could bind to the Kirsten rat sarcoma (KRAS) G12C mutant and cause its inhibition to promote apoptosis in H23 cells. **Materials and Methods:** NGN was docked with mutant KRAS protein followed by molecular dynamics simulation. HDOCK was used to analyse the influence of NGN on the KRAS and PI3K protein-protein docking. We checked the ultramorphological structure of the cells. A 2D-QSAR study was carried out to predict the activity of NGN. **Results:** We observed that NGN bound stably to the mutant KRAS. NGN showed steady RMSF and RMSD values, good structural stability, and favourable MM/PBSA values. NGN interfered in the binding of KRAS and PI3K. NGN treated cells showed hallmarks of apoptotic cell death. The predictive  $pIC_{50}$  value was found to be 7.39 for NGN against KRAS. NGN cleared all the drug filters. **Conclusion:** We conclude that NGN could bind to the mutant KRAS potentially inhibiting KRAS. That affects the PI3K/Akt pathway activation leading to apoptosis in the NCI-H23 cells.

**Keywords:** NSCLC, KRAS, Naringenin, Docking, Apoptosis, QSAR.

Abani Kumar Patar,  
Lakhon Kma, Jitul Barman,  
Shekhar Ghosh, Taranga  
Jyoti Baruah\*

Department of Biochemistry, Assam  
Royal Global University, Guwahati,  
Assam, INDIA.

## Correspondence

Dr. Taranga Jyoti Baruah

Department of Biochemistry,  
Assam Royal Global University,  
Guwahati-781035, Assam, INDIA.  
Email id: taranga18@gmail.com  
ORCID ID: 0000-0002-8819-2232

## History

- Submission Date: 05-04-2022;
- Review completed: 12-05-2022;
- Accepted Date: 14-06-2022.

DOI : 10.5530/pres.14.3.37

## Article Available online

<https://www.phcogres.com/v14/i3>

## Copyright

© 2022 Phcog.Net. This is an open-access article distributed under the terms of the Creative Commons Attribution 4.0 International license.

## INTRODUCTION

Non-small cell lung cancer (NSCLC) is one of the most common forms of cancer worldwide and has a mortality rate of almost 26%.<sup>[1]</sup> The most commonly altered proteins in the adenocarcinomas subtype of NSCLC include epidermal growth factor receptor (EGFR), Kirsten rat sarcoma (KRAS), the Phosphatidylinositol 3-kinase/Protein Kinase B (PI3K/Akt) pathway components, Mesenchymal epithelial transition (MET), ROS proto-oncogene 1 (ROS1) and B-Raf protooncogene (BRAF). These proteins also happen to be the prime candidates for targeted therapy.<sup>[1]</sup> There are FDA approved inhibitors of EGFR, the PI3K/Akt pathway components, and ROS1 that are being used as a replacement for chemotherapy.<sup>[2]</sup> Although tumours respond well to the initial treatment, the cancer cells invariably attain resistance against these inhibitors. Resistance is associated with mutations in MET, KRAS, and epithelial to mesenchymal transition (EMT).<sup>[2]</sup>

The NCI-H23 (H23) cell line is a lung adenocarcinoma cell line containing KRAS G12C mutant protein.<sup>[3]</sup> The G12C mutations allow the KRAS protein to be constantly bound to GTP arising from a loss of GTPase activity. That results in constant activation of the KRAS-PI3K/Akt signalling cascade, leading to an unrestrained proliferation of cancer cells. The GTP bound KRAS directly binds to the Ras Binding Domain of the PI3K 110 $\alpha$  subunit causing its

activation.<sup>[4]</sup> KRAS-PI3K/Akt signalling promotes epithelial to mesenchymal transition (EMT), which allows cancer cells to achieve metastatic potential, facilitating resistance to chemotherapeutic drugs.<sup>[5]</sup> Central to the KRAS-PI3K/Akt signalling chain is the activation of the Akt protein that enables tumour resistance by suppressing apoptosis, promoting the expression of anti-apoptotic proteins.<sup>[5]</sup> In H23 cells, the KRAS G12C mutant promotes the PI3K/Akt signalling. That makes H23 cells resistant to regular chemotherapy treatments.<sup>[6]</sup> Recently, sotorasib has become the first KRAS specific inhibitor to be approved by the FDA against NSCLC. On the flip side, almost 70% of the patients in the clinical trial showed adverse side effects that included grade 3 and grade 4 events and a median survival of 12 months.<sup>[7]</sup>

We turned to flavonoids to look for a safer alternative to sotorasib. We chose the flavonoid naringenin (NGN) as it has reported anti-cancer activities. NGN is a component of commonly consumed fruits and vegetables. Studies have proven NGN to be safe for oral consumption.<sup>[8]</sup> We observed from our *in-silico* study that NGN bound steadily to the KRAS G12C mutant. Our *in-vitro* studies showed the occurrence of apoptosis in the NGN treated H23 cells. In this regard, we propose NGN as a potential inhibitor of

**Cite this article:** Patar AK, Kma L, Barman J, Ghosh S, Baruah TJ. KRAS G12C as a Target of Naringenin for Inducing Cell Death in NCI-H23 Cells. *Pharmacogn Res.* 2022;14(3):256-62.



KRAS G12C and advocate further studies on its inhibitory effect on the G12C mutant of KRAS.

## MATERIALS AND METHODS

### Preparation of Ligand and Protein for Docking

The 3D structure of NGN was downloaded from the PubChem server.<sup>[9]</sup> The Open Babel software was used to convert the .sdf files into .pdb format.<sup>[10]</sup> The Autodock application of MGL tools was then utilized to generate the final .pdbqt file format. The .pdb file for the KRAS wild type and mutant proteins were converted to .pdbqt files using the Autodock function.<sup>[11]</sup>

### Docking using Autodock 4.0

For carrying out the docking investigation, the amino acids involved in protein functioning were incorporated within the grid box set at 60 × 60 × 60 Å (x, y, and z). The grid spacing was kept at 0.5 Å. Autodock analysis was carried out.<sup>[11]</sup> Discovery studio software was used to obtain 2D images of the flavonoid-protein docking.

### Conserved Domain

We utilised the Conserved domain database of the NCBI website<sup>[12-15]</sup> to analyse the amino acids involved in carrying out critical functions of the KRAS protein as per the protocol mentioned by Yang *et al.*<sup>[16]</sup>

### Molecular Dynamics Simulation

The molecular dynamics (MD) simulation has been conducted for the NGN-KRAS complex using GROMACS 2018.3 for a time scale of 100 ns. The AMBER99SB-ILDN force field<sup>[17]</sup> was used to perform the simulation. Force field topology of ligand and protein was obtained using ACPYPE and pdb2gmx programs respectively.<sup>[18]</sup> A 1 nm water cube was used to solvate the protein-ligand complex. The system was neutralised using 0.15 M NaCl. The energy minimization was performed using the steepest descent and conjugate gradient for 50,000 steps. Finally, 100ns of production MD run was performed. The pressure of the protein-ligand system was maintained at 1 bar. The analyses were performed using GROMACS 2018.3 package<sup>[19]</sup> and, the plots were viewed using GRACE.<sup>[19]</sup>

### MM/PBSA based free Energy Calculation

The MM/PBSA calculation for determining binding energy was performed using the g\_mmpbsa tool was used. A python script MmPbSaStat.py, which is provided in the g\_mmpbsa package, was used to calculate the binding energy components of protein-ligand binding.<sup>[20]</sup>

### Protein-protein Docking Study

We performed protein-protein interaction studies of the mutant KRAS and the Ras Binding Domain (RBD) of PI3K protein in the absence and presence of NGN, based on a previous study by Basu *et al.*<sup>[21]</sup> with minor modifications. We used the HDock webserver for carrying out the study.<sup>[22-26]</sup>

### Cell Culture

We procured the NSCLC cell line NCI-H23 (H23) from the National Centre of Cell Science, Pune, India. The cells were maintained in a culture media containing RPMI 1640 (Invitrogen, USA), 2mM L-glutamine (Invitrogen, USA), 10% fetal bovine serum (FBS) (Himedia, India) and 0.1% antibiotics (Invitrogen, USA).

### Ultrastructural Studies

To check for apoptosis, we performed the ultrastructure analysis of the H23 cells. We followed the protocol of Hayat *et al.*<sup>[27]</sup> with minor

modifications for preparing the cells for ultrastructural study. At the end of the 24 hr treatment period, we trypsinized the cells and washed them with PBS. Cell fixation was achieved with Karnovsky's fixative and 1% osmium tetroxide followed by dehydration. Cells were embedded in a mixture of embedding medium and propylene oxide followed by sectioning and staining with uranyl acetate and viewed under Transmission Electron Microscope (TEM).

### 2D-Quantitative-structure activity relationship (QSAR) study

For this QSAR study, a dataset of 37 compounds with inhibitory activity (IC<sub>50</sub>) against the KRAS protein and also a structural file of NGN was retrieved from the ChEMBL database. The IC<sub>50</sub> value of inhibitors was converted to the pIC<sub>50</sub>(-LogIC<sub>50</sub>). The conversion of 2D structure to 3D by Marvin Sketch software. Determination of 2D descriptors by PaDEL-Descriptor software version 2.20 was performed.<sup>[28]</sup> The data pretreatment, dataset division, model building, model validation, and prediction steps of QSAR studies were performed using the Drug Theoretics and Cheminformatics (DTC)-QSAR software. Dataset was divided into training and test datasets by applying Kennard-Stone's algorithm.<sup>[29]</sup> The QSAR model, generated by the multiple linear regression (MLR) analysis, was validated and used for the prediction of the pIC<sub>50</sub> value of inhibitors as well as NGN. Internal and external validation was carried as mentioned by Tropsha.<sup>[30]</sup> Moreover, a Y-Randomization test was performed to ensure the robustness of the developed model.

### Drug likeliness analysis

NGN was checked for its drug-likeness ability using the Swiss ADME webserver.<sup>[31]</sup>

## RESULTS

From our docking study, we observed that NGN had a better binding affinity to the KRAS G12C mutant protein as compared to the wild type KRAS protein (Table 1, Figure 1). NGN formed several hydrogen bonds with both the wild type and mutant KRAS proteins. The molecular dynamic simulation showed a gradual reduction of the system's potential energy during the time period of simulation (Figure 2a). The solvent accessible surface area (SASA) of the complex remained approximately at 90 nm<sup>2</sup> during the time period of the simulation (Figure 2b). The radius of gyration (Rg) also stayed constant at 1.55 nm during the entire period of the simulation (Figure 2c). The Root mean square deviation (RMSD) values of the Ca carbons of the 4LUC (G12C KRAS) protein showed a steady RMSD value of 0.1 nm beyond 40 ns (Figure 3a). The RMSD values of the complex when NGN was the reference alignment molecule showed a steady value of 0.1 nm post 30 ns till the end of the simulation (Figure 3b). The amino acids ranging from 60 to 73 showed higher Root mean square fluctuation (RMSF) values. The highest RMSF values stood at 0.2 nm and it was observed in the amino acid residues 63-65 (Figure 4a). The analysis of the protein-NGN H-bond interaction (Figure 4b) showed the presence of 5 H-bonding interactions all through the duration of the simulation. The MM/PBSA analysis revealed the

**Table 1: Docking details of NGN with the KRAS wild type and the KRAS G12C mutant protein.**

Sl. No	Protein	PDB ID	Binding energy (kcal/mol)	Inhibition constant (μM)
1	KRAS protein	4LPK	-7.41	3.72
2	Mutant KRAS protein	4LUC	-7.74	2.11

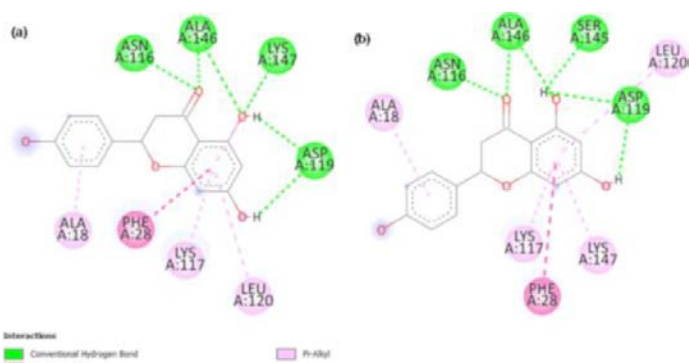


**Figure 1:** 2D representation of the docking of NGN with (a) wild type KRAS protein, (b) mutant KRAS protein.

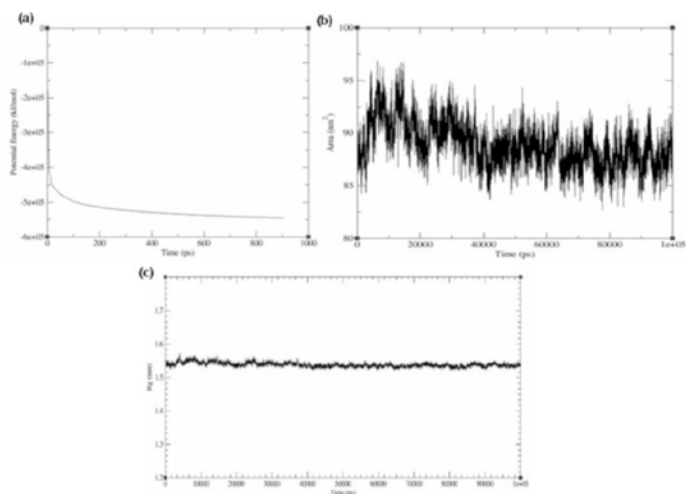


**Figure 2:** Graphs representing (a) potential energy over a time scale of 1000 ps, (b) solvent accessible surface area, and (c) radius of gyration; of the mutant KRAS-NGN complex. (b) and (c) were checked over a time scale of 10000 ps.

energy values of the different types of interactions between the mutant KRAS protein and NGN (Table 2).

From our protein-protein docking studies (Table 3), we observed that the presence of NGN caused a lowering of the docking score between the mutant KRAS and the RBD of the PI3K 110 $\alpha$  subunit. The ultramorphological analysis showed the presence of the standard apoptotic markers in the NGN treated cells like chromatin condensation, membrane blebbing, apoptotic body formation, cytoplasmic vesicle formation and nuclear fragmentation (Figure 5).<sup>[32]</sup> The untreated H23 cells didn't show any of the apoptotic markers.

Based on the training dataset containing 26 inhibitors (Table 4), QSAR model was developed using 2D descriptors calculated solely from the structure of these chemical compounds. The QSAR model in terms of MLR was generated as:  $pIC_{50} = -3.4957 - 3.3411 \cdot AATSC7s - 0.0009 \cdot ATSC6m + 0.1911 \cdot AATSC0v$ . The QSAR model indicated that the dependent variable,  $pIC_{50}$ , has a significant correlation with the three descriptors namely AATSC7s, ATSC6m, and AATSC0v. As observed in the response plot (Figure 6a), a good correlation is evident between the experimentally observed  $pIC_{50}$  values and the predicted  $pIC_{50}$  values ranging from 5.07 to 7.94 and from 6.76 to 7.60 in the case of training and test dataset respectively. The statistical metrics  $Q^2_{(LOO)}$ ,  $R^2$ ,  $R^2_{(adjusted)}$

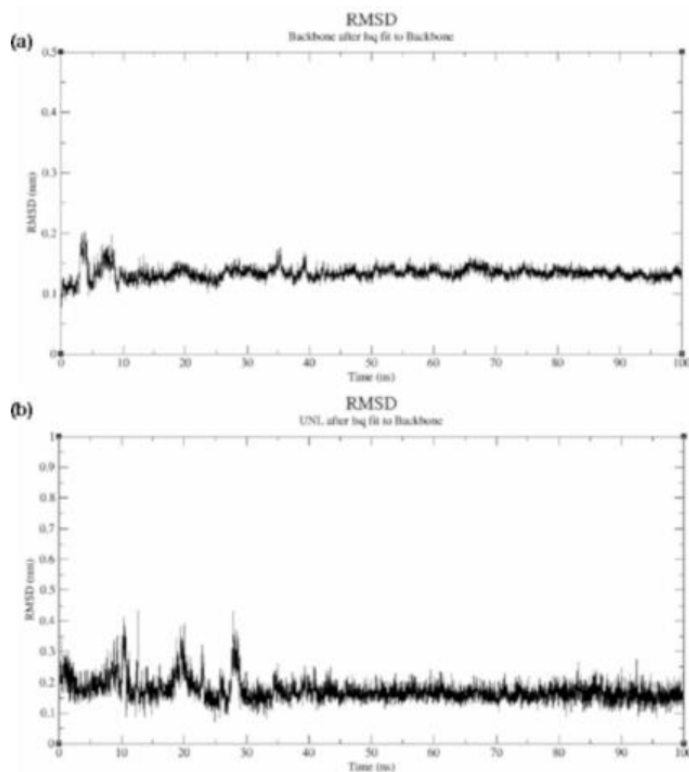


**Figure 3:** Graphs representing (a) RMSD of the Ca carbons of the mutant KRAS protein, (b) RMSD values of the complex when NGN was used as a reference alignment molecule. Both the runs were carried out over a time scale of 100 ns.

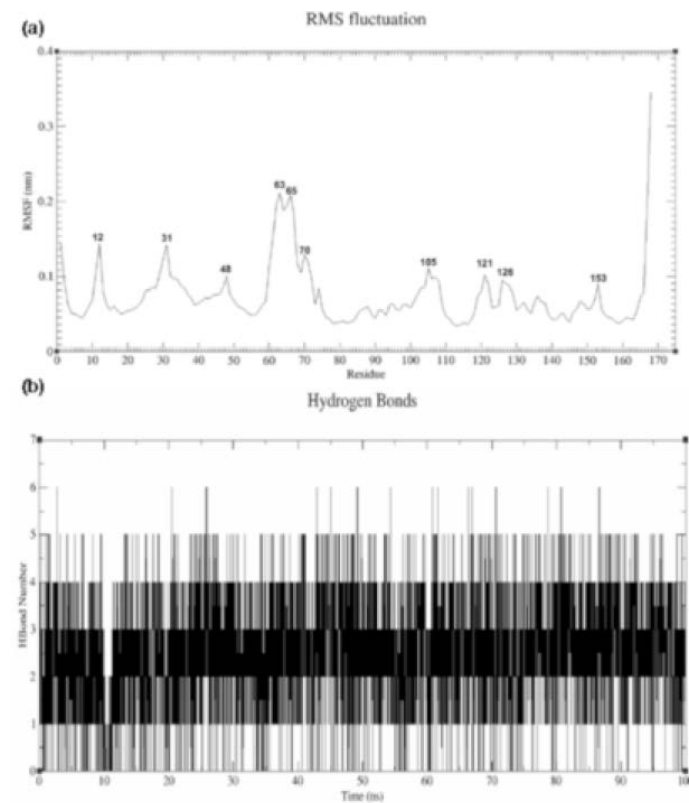


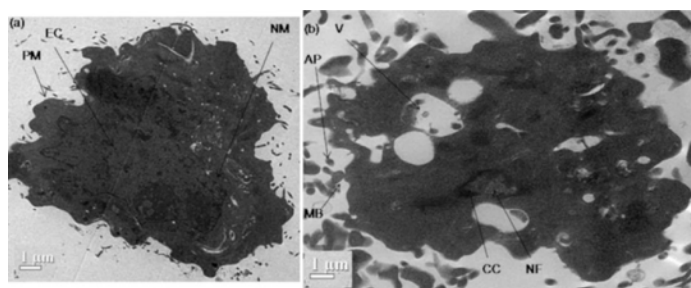
**Figure 4:** Graphs representing (a) RMSF values indicating the flexibility of amino acid residues, (b) average number of H-bonds between mutant KRAS-NGN complex.

**Table 2: Energies associated with mutant KRAS and NGN binding.**

Sl. No	Energetic components	Energy (kJ/mol)
1	van der Waal's energy	-158.237 ± 15.043
2	Electrostatic energy	-19.427 ± 8.463
3	Polar salvation energy	114.394 ± 16.987
4	SASA energy	-13.931 ± 0.892

**Table 3: Protein-protein binding energy obtained in the absence and presence of NGN.**

Protein-protein complex	NGN	Docking score
G12C KRAS-PI3K	Absent	-224.98
G12C KRAS-PI3K	Present	-205.69

**Figure 5:** TEM micrographs showing (a) untreated cell showing intact plasma membrane (PM), evenly distributed chromatin (EC), intact nuclear membrane (NM), (b) NGN treated cell showing nuclear fragmentation (NF), chromatin condensation (CC), vesicle formation (V), membrane blebbing (MB) and apoptotic bodies (AP).

and SEE relating to the internal predictability quality of the model showed the score of 0.8221, 0.8761, 0.8592 and 0.3427 respectively. In Y-Randomization test against the model, average  $R^2$  value of 0.152349 and average  $Q^2_{(LOO)}$  value of -0.19934 were resulted (Table 5). Upon the external validation of the model, results obtained were  $Q^2_{F1} = 0.6713$ ,  $Q^2_{F2} = 0.5126$ , average  $Rm^2_{(Test)} = 0.5701$ ,  $\Delta Rm^2_{(Test)} = 0.4912$ , and  $MAE = 0.1895$ . It is evident from the residual plot (Figure 6b) that the propagation of the residuals for the predicted values of  $pIC_{50}$  for both the training and test sets against the observed  $pIC_{50}$  is random on both sides of zero, indicating no systematic errors in the model. The prediction of inhibitory activity of NGN against the KRAS by the QSAR model resulted in the  $pIC_{50}$  value of 7.39 (Table 6). And lastly, NGN cleared all the drug likeliness filters (Table 7).

## DISCUSSION

We have previously shown that NGN had a cytotoxic effect upon the H23 cells with an  $IC_{50}$  value of approximately 100  $\mu M$ . We have demonstrated the inhibition of colony formation of H23 cells by NGN and the lack of any adverse effects on the fibroblast cell line HEK293T that harbours a wildtype KRAS.<sup>[33-34]</sup> NGN is bound to several critical amino acids in the KRAS protein. From the conserved sequence database of NCBI, the amino acid residues ALA 18, ASN 116, LYS 117, ASP 119, LEU 120, ALA 146, and LYS 147 were found to be present in the GTP/Mg<sup>2+</sup> binding site. Obstruction of the binding of GTP to the KRAS protein has proven to inhibit the actions of the downstream effector proteins like RAF and PI3K.<sup>[35]</sup> The gradual reduction of the system's energy indicated that the

**Table 4: Observed  $pIC_{50}$ , 2D descriptor, and predicted  $pIC_{50}$  values of training and test dataset inhibitors of KRAS.**

SI. No	ChEMBL ID	Observed $pIC_{50}$	Training dataset			Predicted $pIC_{50}$
			2D Descriptors	ATATSC7s	ATATSC6m	
1	CHEMBL4450519	7.18	-0.28033	13.28155	50.61602	7.10
2	CHEMBL4591772	7.25	-0.25221	47.93716	51.7728	7.20
3	CHEMBL4467413	7.29	-0.40978	37.91749	50.09632	7.41
4	CHEMBL4527861	7.42	-0.29218	-794.503	48.428	7.41
5	CHEMBL4515333	6.66	-0.37306	96.43433	47.93845	6.83
6	CHEMBL4528930	7.96	-0.26442	-879.51	49.27562	7.56
7	CHEMBL4539214	5.48	0.224509	-95.0645	49.97589	5.40
8	CHEMBL4573279	5.09	0.195883	98.70915	49.16569	5.16
9	CHEMBL4466063	7.19	-0.29252	-808.101	49.27562	7.59
10	CHEMBL4517656	6.89	-0.24163	-662.628	47.46254	6.95
11	CHEMBL4441771	5.75	0.160064	100.7661	50.9267	5.62
12	CHEMBL4549665	7.16	-0.24818	-262.241	49.52021	7.02
13	CHEMBL4439782	7.55	-0.23852	-114.794	50.56848	7.06
14	CHEMBL4449810	7.1	-0.14667	19.78087	51.12581	6.75
15	CHEMBL4535757	7.33	-0.21229	0.746908	51.28108	7.01
16	CHEMBL4467518	7.44	-0.26114	-777.451	50.09632	7.61
17	CHEMBL4554946	7.44	-0.34574	-449.27	48.42235	7.30
18	CHEMBL4588277	6.66	-0.18316	135.517	52.58831	7.05
19	CHEMBL4454645	7.6	-0.19796	-685.81	49.72371	7.25
20	CHEMBL4452622	6.36	-0.27846	622.545	49.82956	6.42
21	CHEMBL4553629	7.6	-0.44502	-642.283	49.19141	7.94
22	CHEMBL4456801	5.45	0.242115	26.79967	49.1768	5.07
23	CHEMBL4434842	6.08	-0.13557	37.30794	46.74925	5.86
24	CHEMBL4514914	7.36	-0.34063	-214.827	49.72371	7.33
25	CHEMBL4516179	6.84	-0.28365	-224.974	50.63846	7.32
26	CHEMBL4450657	4.24	0.24099	-22.6228	49.33894	5.15
Test dataset						
1	CHEMBL4517656	6.47	-0.18686	-52.4649	50.18305	6.76
2	CHEMBL4476789	7.2	-0.33429	-57.3308	49.64633	7.16
3	CHEMBL4578214	6.89	-0.18686	-52.4649	50.18305	6.76
4	CHEMBL4468009	6.96	-0.28417	-289.237	49.23872	7.11
5	CHEMBL4469638	7.17	-0.26967	-824.281	48.13017	7.31
6	CHEMBL4465551	7.55	-0.20934	-919.223	50.24872	7.60
7	CHEMBL4452137	7.28	-0.30672	-137.526	49.25224	7.06
8	CHEMBL4464232	7.05	-0.18124	-791.778	49.09783	7.17
9	CHEMBL4438343	6.9	-0.25497	-745.41	48.40056	7.24
10	CHEMBL4214264	6.7	-0.14357	-462.464	49.28154	6.80
11	CHEMBL4450041	6.85	-0.30267	-755.196	48.13017	7.36

system was close to its natural structure (Figure 2a).<sup>[36]</sup> The steady values of solvent accessible surface area (SASA) and radius of gyration showed the integrity of the protein folds during the time course of the simulation.<sup>[37]</sup> The constant RMSD value in the range of 0.1 nm indicates a good binding interaction between NGN and the mutant KRAS. The higher RMSF values of the amino acids in position range of 60-73 indicated

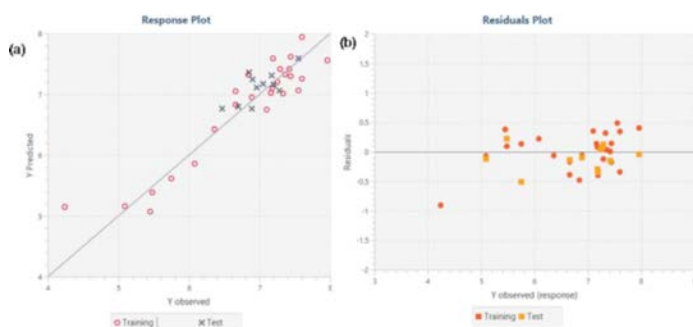


**Figure 6:** Graphs showing (a) response plot of the predicted  $pIC_{50}$  values against the observed  $pIC_{50}$  values of training and test dataset inhibitors of KRAS, (b) residuals plot of standardized residuals against the observed  $pIC_{50}$  values of KRAS inhibitors.

**Table 5: Y-Randomization test for the QSAR model.**

Sl. No	Models	R <sup>2</sup>	Q <sup>2</sup> <sub>(LoO)</sub>
1	ORIGINAL	0.876057	0.82209
2	RANDOM	0.047233	-0.32519
3	RANDOM	0.237183	-0.09628
4	RANDOM	0.120591	-0.15546
5	RANDOM	0.154577	-0.33325
6	RANDOM	0.191125	-0.14989
7	RANDOM	0.18213	-0.20728
8	RANDOM	0.173233	-0.10949
9	RANDOM	0.134849	-0.21464
10	RANDOM	0.157336	-0.23113
11	RANDOM	0.125229	-0.17082

Summary:

Average R<sup>2</sup> (Random Models): 0.152349

Average Q<sup>2</sup><sub>(LoO)</sub> (Random Models): -0.19934

**Table 6: 2D descriptor values and predicted  $pIC_{50}$  value of NGN.**

CHEMBL ID	NGN			Predicted $pIC_{50}$
	2D Descriptors			
	AATSC7s	ATSC6m	AATSC0v	
CHEMBL9352	-0.63937	273.2946	46.98576	7.39

**Table 7: Drug like lines of NGN.**

Lipinski filter	Ghose filter	Veber filter	Egan filter	Muegge filter
Cleared	Cleared	Cleared	Cleared	Cleared

higher flexibility of those residues.<sup>[38]</sup> These amino acids with higher flexibility comprise the GEF interaction site. Considering that higher RMSF values have correlated with lower catalytic efficiency,<sup>[39]</sup> our RMSF results may be indicative of impaired nucleotide exchange capacity of the mutant KRAS protein when bound to NGN.<sup>[39]</sup> We observed the regular presence of 5 H-bonds between NGN and the mutant KRAS protein. Previous workers have reported almost the same or lower number of H-bond interactions between the mutant KRAS and the compounds under study.<sup>[40]</sup> The MM/PBSA results confirmed the favourable binding,

thermodynamic stability and inhibitory potency in the binding between KRAS and NGN.<sup>[41]</sup>

The docking results between the mutant KRAS and the Receptor binding domain (RBD) of PI3K indicated the hampering of the binding interactions between the mutant KRAS with the RBD of the PI3K 110 $\alpha$  subunit.<sup>[21]</sup> Our previous study confirms this inference as we had observed a significant reduction in the levels of pAkt protein in the NGN treated group compared to the untreated cancer cells.<sup>[34]</sup> The presence of apoptosis markers in the NGN treated cells correlates with our previously reported increase in the caspase-3 activity in the NGN treated H23 cells.<sup>[34]</sup> Thus we can hypothesize that treatment with NGN could potentially bind with KRAS, inhibiting the activation of the PI3K/Akt pathway and promoting apoptotic cell death in H23 cells.

In this study, AATSC7s, ATSC6m, and AATSC0v, all 2D autocorrelation descriptors, were found to be highly significant. The model highlights the positive contribution of AATSC0v and the negative contribution of AATSC7s and ATSC6m on the activity. The  $pIC_{50}$  value is augmented in response to the increase of AATSC0v whereas it is diminished in response to the increase of AATSC7s and ATSC6m. The acceptability of the model in terms of stability, predictive ability, and fitness can be ascertained from the high values of R<sup>2</sup> and Q<sup>2</sup><sub>(LoO)</sub> and low value of SEE.<sup>[42]</sup> It is also clear that the external predictive quality of the model is good as confirmed from the results of statistical analysis of the test dataset. The Y-Randomization test involves the repeating of a process in which the dependent variable vectors are shuffled randomly while keeping the independent variable vectors unaltered to build new models.<sup>[43]</sup> The lower value of average R<sup>2</sup> and average Q<sup>2</sup><sub>(LoO)</sub> of these new models indicates that the current model is robust and not an outcome of chance.<sup>[44]</sup> Interestingly, the predictive  $pIC_{50}$  value of NGN computed by the QSAR model is relatively higher as well as comparable to observed  $pIC_{50}$  value of selected KRAS inhibitors in this study, implying the significant possible action of NGN against the KRAS activity. The ability of NGN to clear all the drug filters further highlighted the suitability and safety profile of NGN for future clinical success.<sup>[45]</sup>

## CONCLUSION

Our study indicates that the cytotoxicity of NGN towards H23 cells can be attributed to NGN potentially binding to the mutant KRAS G12C protein harboured in the H23 cells. NGN caused interference in the binding between the KRAS G12C protein and the PI3K protein inhibiting the latter's activity. That lead to PI3K/Akt pathway inhibition and the subsequent apoptotic activity in the NGN treated cells. NGN showed a favourable  $pIC_{50}$  value against KRAS protein, and NGN also cleared all the drug likeliness filters. Thus NGN should be further studied as a potential candidate for the treatment of G12C KRAS harbouring cancers.

## ACKNOWLEDGEMENT

This work was supported by funds provided by Department of Science and Technology-Science and Engineering Research Board, New Delhi, India to Dr. L. Kma (SERB/F/3862/2014-15) and grant from University Grants Commission, New Delhi, India under Departmental Research Support-II and Departmental Research Support-III program to the Department of Biochemistry, NEHU, Shillong, India. Authors would also like to acknowledge Department of Biochemistry, North Eastern Hill University, Assam Royal Global University, and Mr. Biologist Pvt Ltd for facilitating the work.

## CONFLICT OF INTEREST

The authors declare that there is no conflict of interest.

## ABBREVIATIONS

**NSCLC:** Non Small Cell Lung Cancer; **EGFR:** Epidermal Growth Factor Receptor; **KRAS:** Kirsten Rat Sarcoma; **PI3K/Akt:** Phosphatidylinositol 3 kinase/Protein Kinase B; **MET:** Mesenchymal Epithelial Transition; **ROS1:** ROS proto-oncogene1; **BRAF:** B-Raf Proto-oncogene; **EMT:** Epithelial to Mesenchymal Transition; **NGN:** Naringenin; **RMSD:** Root Mean Square Deviation; **RMSF:** Root Mean Square Fluctuation; **SASA:** Solvent Accessible Surface Area; **QSAR:** Quantitative-Structure Activity Relationship; **MM/PBSA:** Molecular Mechanics energies combined with the Poisson–Boltzmann or generalized Born and Surface Area continuum solvation.

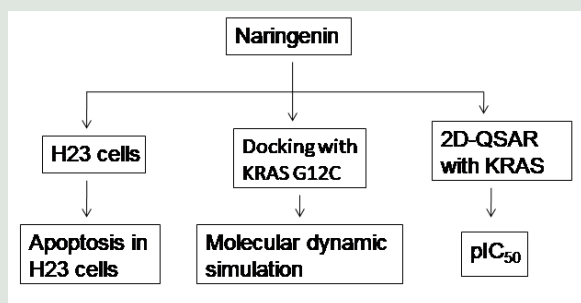
## REFERENCES

- Majeed U, Manochakian R, Zhao Y, Lou Y. Targeted therapy in advanced non-small cell lung cancer: current advances and future trends. *J Hematol Oncol*. 2021 Jul 8;14(1):108. doi: 10.1186/s13045-021-01121-2, PMID 34238332.
- Yuan M, Huang LL, Chen JH, Wu J, Xu Q. The emerging treatment landscape of targeted therapy in non-small-cell lung cancer. *Signal Transduct Target Ther*. 2019 Dec 17;4:1-14.
- Molina-Arcas M, Moore C, Rana S, Maldegem van F, Mugarza E, Romero-Clavijo P, Herbert E, Horswell S, Li LS, Janes MR, Hancock DC, Downward J. Development of combination therapies to maximize the impact of KRAS-G12C inhibitors in lung cancer. *Sci Transl Med*. 2019 Sep 18;11(510):1-33. doi: 10.1126/scitranslmed.aaw7999, PMID 31534020.
- Krygowska AA, Castellano E. PI3K: A crucial piece in the RAS signaling puzzle. *Cold Spring Harb Perspect Med*. 2018 Jun 1;8(6):1-19. doi: 10.1101/cshperspect.a031450, PMID 28847905.
- Cuesta C, Arévalo-Alameda C, Castellano E. The importance of being PI3K in the RAS signaling network. *Genes (Basel)*. 2021 Jul 19;12(7):1-40. doi: 10.3390/genes12071094, PMID 34356110.
- Sunaga N, Shames DS, Girard L, Peyton M, Larsen JE, Imai H, Soh J, Sato M, Yanagitani N, Kaira K, Xie Y, Gazdar AF, Mori M, Minna JD. Knockdown of oncogenic KRAS in non-small cell lung cancers suppresses tumor growth and sensitizes tumor cells to targeted therapy. *Mol Cancer Ther*. 2011 Feb;10(2):336-46. doi: 10.1158/1535-7163.MCT-10-0750, PMID 21306997.
- Hong DS, Fakhri MG, Strickler JH, Desai J, Durm GA, Shapiro GI, Falchook GS, Price TJ, Sacher A, Denlinger CS, Bang YJ, Dy GK, Krauss JC, Kuboki Y, Kuo JC, Coveler AL, Park K, Kim TW, Barlesi F, Munster PN, Ramalingam SS, Burns TF, Meric-Bernstam F, Henary H, Ngang J, Ngarmchamnanrith G, Kim J, Houk BE, Canon J, Lipford JR, Friberg G, Lito P, Govindan R, Li BT. KRAS<sup>G12C</sup> inhibition with Sotorasib in advanced solid tumors. *N Engl J Med*. 2020 Sep 24;383(13):1207-17. doi: 10.1056/NEJMoa1917239, PMID 32955176.
- Rebello CJ, Beyl RA, Lertora JLL, Greenway FL, Ravussin E, Ribnicky DM, Poulev A, Kennedy BJ, Castro HF, Campagna SR, Coulter AA, Redman LM. Safety and pharmacokinetics of naringenin: A randomized, controlled, single-ascending-dose clinical trial. *Diabetes Obes Metab*. 2020 Jan;22(1):91-8. doi: 10.1111/dom.13868, PMID 31468636.
- Kim S, Thiessen PA, Bolton EE, Chen J, Fu G, Gindulyte A, Han L, He J, He S, Shoemaker BA, Wang J, Yu B, Zhang J, Bryant SH. PubChem Substance and Compound databases. *Nucleic Acids Res*. 2016 Jan 4;44(D1):D1202-13. doi: 10.1093/nar/gkv951, PMID 26400175.
- O'Boyle NM, Banck M, James CA, Morley C, Vandermeersch T, Hutchison GR. Open Babel: an open chemical toolbox. *J Cheminform*. 2011 Oct 7;3:33. doi: 10.1186/1758-2946-3-33, PMID 21982300.
- Forli S, Huey R, Pique ME, Sanner MF, Goodsell DS, Olson AJ. Computational protein-ligand docking and virtual drug screening with the AutoDock suite. *Nat Protoc*. 2016 May;11(5):905-19. doi: 10.1038/nprot.2016.051, PMID 27077332.
- Lu S, Wang J, Chitsaz F, Derbyshire MK, Geer RC, Gonzales NR, Gwadz M, Hurwitz DI, Marchler GH, Song JS, Thanki N, Yamashita RA, Yang M, Zhang D, Zheng C, Lanczycki CJ, Marchler-Bauer A. CDD/SPARCLE: the conserved domain database in 2020. *Nucleic Acids Res*. 2020 Jan 8;48(D1):D265-8. doi: 10.1093/nar/gkz991, PMID 31777944.
- Marchler-Bauer A, Bryant SH. CD-Search: protein domain annotations on the fly. *Nucleic Acids Res*. 2004 Jul 1;32(Web Server issue);Web Server Issue:W327-31. doi: 10.1093/nar/gkh454, PMID 15215404.
- Marchler-Bauer A, Derbyshire MK, Gonzales NR, Lu S, Chitsaz F, Geer LY, Geer RC, He J, Gwadz M, Hurwitz DI, Lanczycki CJ, Lu F, Marchler GH, Song JS, Thanki N, Wang Z, Yamashita RA, Zhang D, Zheng C, Bryant SH. CDD: NCBI's conserved domain database. *Nucleic Acids Res*. 2015 Jan;43(Database issue);D222-6. doi: 10.1093/nar/gku1221, PMID 25414356.
- Marchler-Bauer A, Bo Y, Han L, He J, Lanczycki CJ, Lu S, Chitsaz F, Derbyshire MK, Geer RC, Gonzales NR, Gwadz M, Hurwitz DI, Lu F, Marchler GH, Song JS, Thanki N, Wang Z, Yamashita RA, Zhang D, Zheng C, Geer LY, Bryant SH. CDD/SPARCLE: functional classification of proteins via subfamily domain architectures. *Nucleic Acids Res*. 2017 Jan 4;45(D1):D200-3. doi: 10.1093/nar/gkw1129, PMID 27899674.
- Yang M, Derbyshire MK, Yamashita RA, Marchler-Bauer A. NCBI's conserved domain database and tools for protein domain analysis. *Curr Protoc Bioinformatics*. 2020 Mar;69(1):e90. doi: 10.1002/cpbi.90, PMID 31851420.
- Lindorff-Larsen K, Piana S, Palmo K, Maragakis P, Klepeis JL, Dror RO, Shaw DE. Improved side-chain torsion potentials for the Amber ff99SB protein force field. *Proteins*. 2010 Jun;78(8):1950-8. doi: 10.1002/prot.22711, PMID 20408171.
- Sousa da Silva AW, Vranken WF, ACPYPE, AnteChamber P. Ython parser interface. *BMC Res Notes*. 2012 Jul 23;3:67:1-8.
- Abraham MJ, Murtola T, Schulz R, Páll S, Smith JC, Hess B, Lindahl E. GROMACS: high performance molecular simulations through multi-level parallelism from laptops to supercomputers. *SoftwareX*. 2015 Sep;1(2):19-25. doi: 10.1016/j.softx.2015.06.001.
- Kumari R, Kumar R Open Source Drug Discovery Consortium, Open Source Drug Discovery Consortium, Lynn A. g\_mmpbsa—a GROMACS tool for high-throughput MM-PBSA calculations. *J Chem Inf Model*. 2014 Jul 28;54(7):1951-62. doi: 10.1021/ci500020m, PMID 24850022.
- Basu A, Sarkar A, Maulik U. Molecular docking study of potential phytochemicals and their effects on the complex of SARS-CoV2 spike protein and human ACE2 [sci rep:17699]. *Sci Rep*. 2020;10(1):17699. doi: 10.1038/s41598-020-74175-4, PMID 33077836.
- Huang SY, Zou X. An iterative knowledge-based scoring function for protein-protein recognition. *Proteins*. 2008 Aug;72(2):557-79. doi: 10.1002/prot.21949, PMID 18247354.
- Huang SY, Zou X. A knowledge-based scoring function for protein-RNA interactions derived from a statistical mechanics-based iterative method. *Nucleic Acids Res*. 2014 Apr;42(7):e55. doi: 10.1093/nar/gku077, PMID 24476917.
- Yan Y, Wen Z, Wang X, Huang SY. Addressing recent docking challenges: A hybrid strategy to integrate template-based and free protein-protein docking. *Proteins*. 2017 Mar;85(3):497-512. doi: 10.1002/prot.25234, PMID 28026062.
- Yan Y, Zhang D, Zhou P, Li B, Huang SY. HDock: a web server for protein-protein and protein-DNA/RNA docking based on a hybrid strategy. *Nucleic Acids Res*. 2017 Jul 3;45(W1):W365-73. doi: 10.1093/nar/gkx407, PMID 28521030.
- Yan Y, Tao H, He J, Huang SY. The HDock server for integrated protein-protein docking. *Nat Protoc*. 2020 May;15(5):1829-52. doi: 10.1038/s41596-020-0312-x, PMID 32269383.
- Hayat MA. Basic techniques for transmission electron microscopy. 3rd ed. New York: Academic Press; 1995.
- Yap CW. PaDEL-descriptor: an open source software to calculate molecular descriptors and fingerprints. *J Comput Chem*. 2011 May;32(7):1466-74. doi: 10.1002/jcc.21707, PMID 21425294.
- Kennard RW, Stone LA. Computer-aided design of experiments. *Technometrics*. 1969;11(1):137-48. doi: 10.1080/00401706.1969.10490666.
- Tropsha A. Best practices for QSAR model development, validation, and exploitation. *Mol Inform*. 2010 Jul 12;29(6-7):476-88. doi: 10.1002/minf.201000061, PMID 27463326.
- Daina A, Michielin O, Zoete V. SwissADME: a free web tool to evaluate pharmacokinetics, drug-likeness and medicinal chemistry friendliness of small molecules [sci rep:2017] Mar 3;7:1-13.
- Choudhury Y, Sharan RN. Ultrastructural alterations in liver of mice exposed chronically and transgenerationally to aqueous extract of betel nut: implications in betel nut-induced carcinogenesis. *Microsc Res Tech*. 2010 May;73(5):530-9. doi: 10.1002/jemt.20791, PMID 19839060.
- Lee W, Lee JH, Jun S, Lee JH, Bang D. Selective targeting of KRAS oncogenic alleles by CRISPR/Cas9 inhibits proliferation of cancer cells [sci rep:11879]. *Sci Rep*. 2018;8(1):11879. doi: 10.1038/s41598-018-30205-2, PMID 30089886.
- Baruah TJ, Hauneikhim K, Kma L. Naringenin sensitizes lung cancer NCI-H23 cells to radiation by downregulation of Akt expression and metastasis while promoting apoptosis. *Phcog Mag*. 2020 Aug 28;16(70):S229-S35. doi: 10.4103/pm.pm\_535\_19.
- Pantsar T. The current understanding of KRAS protein structure and dynamics. *Comput Struct Biotechnol J*. 2020;18:189-98. doi: 10.1016/j.csbj.2019.12.004, PMID 31988705.
- Rafael TM, Magnólia de AC, Rômulo Maciel de MF. Introductory chapter. 1st ed; 2021. Rafael TM, Rômulo Maciel de MF, Magnólia C. Homology modeling, homology molecular modeling - perspectives and applications. IntechOpen; 2021.
- Dash R, Ali MC, Dash N, Azad MAK, Hosen SMZ, Hannan MA, Moon IS. Structural and dynamic characterizations highlight the deleterious role of SULT1A1 R213H polymorphism in substrate binding. *Int J Mol Sci*. 2019 Dec 11;20(24):1-22. doi: 10.3390/ijms20246256, PMID 31835852.
- AlZahrani WM, AlGhamdi SA, Zughaibi TA, Rehan M. Exploring the natural compounds in flavonoids for their potential inhibition of cancer therapeutic target MEK1 using computational methods. *Pharmaceuticals (Basel)*. 2022 Feb 3;15(2):1-19. doi: 10.3390/ph15020195, PMID 35215307.
- Xu Y, Meng X. Molecular simulation elaborating the mechanism of 1β-hydroxy alantolactone inhibiting ubiquitin-conjugating enzyme UbcH5s [sci rep:141]. *Sci Rep*. 2020;10(1):141. doi: 10.1038/s41598-019-57104-4, PMID 31924820.
- Aliyar M, Aryapour H, Mahdavi M. *In-silico* predictive identification of K-RasG12V

inhibitors in natural compounds. bioRxiv. 2019. PMID 553149.

41. Rastelli G, Rio Del A, Degliesposti G, Sgobba M. Fast and accurate predictions of binding free energies using MM-PBSA and MM-GBSA. *J Comput Chem.* 2010 Mar;31(4):797-810. doi: 10.1002/jcc.21372, PMID 19569205.
42. Golbraikh A, Tropsha A. Predictive QSAR modeling based on diversity sampling of experimental datasets for the training and test set selection. *Mol Divers.* 2002;5(4):231-43. doi: 10.1023/a:1021372108686, PMID 12549674.
43. Pourbasheer E, Vahdani S, Aalizadeh R, Banaei A, Ganjali MR. QSAR study of polycarboxypeptidase inhibitors by genetic algorithm: multiple linear regressions. *J Chem Sci.* 2015 Jul;127(7):1243-51. doi: 10.1007/s12039-015-0893-z.
44. Mahmud AW, Shallangwa GA, Uzairu A. QSAR and molecular docking studies of 1,3-dioxoisindoline-4-aminoquinolines as potent antiplasmodium hybrid compounds. *Heliyon.* 2020 Mar 2;6(3):e03449. doi: 10.1016/j.heliyon.2020.e03449, PMID 32154412.
45. Hussain N, Kakoti BB, Rudrapal M, Sarwa KK, Celik I, Attah EI, Khairnar *et al.* Bioactive antidiabetic flavonoids from the stem bark of *Cordia dichotoma* Forst.: identification, docking and ADMET studies. *Molbank.* 2021 June 11;2021;2:1-10.

## GRAPHICAL ABSTRACT



## SUMMARY

- This work checked the possibility of naringenin docking with KRAS G12C protein to promote apoptosis in H23 cells.
- Our *in-silico* analysis showed the steady binding of naringenin with the mutant KRAS G12C protein.
- This interaction lead to the promotion of apoptosis in the H23 cells.
- 2D-QSAR analysis also showed a favourable pIC<sub>50</sub> value for naringenin against KRAS protein.

**Cite this article:** Patar AK, Kma L, Barman J, Ghosh S, Baruah TJ. KRAS G12C as A Target of Naringenin for Inducing Cell Death in NCI-H23 Cells. *Pharmacog Res.* 2022;14(3):256-62.